

The Optical Instrumentation of the ATLAS Tile Calorimeter

The ATLAS Tile Calorimeter Community

V. Guarino, T. Le Compte, L. Nodulman, L. E. Price, J. Proudfoot, J. Schlereth, R. Stanek, D. Underwood

Argonne National Laboratory, Argonne, Illinois, USA

K. De, J. Li, M. Sosebee, A. Vartapetian, A. White
University of Texas at Arlington, Arlington, Texas, USA

A. Antonaki, D. Fassouliotis, V. Giakoumopoulou, N. Giokaris, A. Manousakis, C. Vellidis
University of Athens, Athens, Greece

G. Blanchot, M. Bosman, M. Cavalli-Sforza, I. Korolkov, L. Miralles, O. Norniella, X. Portell, O. Salto, M. Volpi
Institut de Fisica d'Altes Energies, Universitat Autònoma de Barcelona, Barcelona, Spain

P. Bednar, I. Fedorko, I. Sykora, S. Tokar, T. Zenis
Comenius University, Bratislava, Slovakia

C. Alexa, V. Boldea, S. Constantinescu, S. Dita, D. Pantea
Institute of Atomic Physics, Bucharest, Romania

K. Anderson, A. Farbin, A. Gupta, M. Hurwitz, F. Merritt, M. Oreglia, J. Pilcher, H. Sanders, M. Shochet, F. Tang, R. Teuscher
University of Chicago, Chicago, Illinois, USA

C. Biscarat, D. Calvet, C. Ferdi, V. Garde, P. Gris, C. Guicheney, R. Lefevre, G. Montarou, D. Pallin, F. Podlyski, P. Rosnet, P. Roy, C. Santoni, L.-P. SAYS, F. Vazeille
LPC Clermont-Ferrand, Université Blaise Pascal / CNRS-IN2P3, Clermont-Ferrand, France

V. Batusov, J. Budagov, J. Khubua (also Tbilisi), Y. Kulchitsky (also Minsk), M. Liablin, Y. Lomakin, S. Maliukov, I. Minashvili, V. Romanov, N. Russakovich, A. Sissakian,
JINR, Dubna, Russia

C. Bromberg, J. Huston, R. Miller, R. Richards
Michigan State University, East Lansing, Michigan, USA

M. Cobal, B. Di Girolamo, I. Efthymiopoulos, O. Gildemeister, P. Grenier, A. Henriques, F. Martin, M. Nessi, G. Schlager, F. Spano
CERN, Geneva, Switzerland

M. David, A. Gomes, A. Maio, C. Marques, J. Pina, J. G. Saraiva, J. Silva, J. Santos
LIP and FCUL Univ. of Lisbon, Portugal

J. Carvalho, J. Pinhao,
LIP and FCTUC Univ. of Coimbra, Portugal

A. Onofre
LIP and Univ. Catolica Figueira da Foz, Portugal

A. Bogush, V. Gilewsky, Yu. Kurochkin, Y. Kulchitsky (also Dubna), I. Satsunkevitch
Institute of Physics, National Academy of Sciences, Minsk, Belarus

P. Kuzhir, V. Rumiantsov, P. Shevtsov, P. Starovoitov
National Centre of Particles and High Energy Physics, Minsk, Belarus

P. Adragna, V. Cavasinni, D. Costanzo, T. Del Prete, A. Dotti, V. Flaminio, A. Lupi, E. Mazzoni, C. Roda, F. Sarri, G. Usai, I. Vivarelli
Pisa University and INFN, Pisa, Italy

T. Davidek, J. Dolejsi, Z. Dolezal, P. Krivkova, R. Leitner, M. Suk, P. Tas, S. Valkar
Charles University in Prague, Prague, Czech Republic

M. Lokajicek, S. Nemecek, L. Pribyl
Institute of Physics, Academy of Sciences of the Czech Republic, Prague, Czech Republic

A. Fenyuk, A. Karyukhin, A. Miagkov, A. Solodkov, O. Solovianov, E. Starchenko, A. Zaitsev, A. Zenine
Institute for High Energy Physics, Protvino, Russia

A. S. Cerqueira, B. C- Ferreira, C. Maidantchik, F. Marroquim, J. M. Seixas, P. Da Silva
COPPE/EE/UFRJ, Rio de Janeiro, Brazil

C. Bohm, S. Holmgren, K. Jon-And, J. Klereborn, M. Ramstedt, B. Sellden
Stockholm University, Stockholm, Sweden

J. Khubua (also Dubna)
HEPI, Tbilisi State Univ., Tbilisi, Georgia

F. Cogswell, R. Downing, D. Errede, S. Errede, M. Haney, T. Junk, V. Simaitis, I. Vichou
University of Illinois, Urbana--Champaign, Illinois, USA

J. Castelo, M. V. Castillo, C. Cuenca, A. Ferrer, E. Fullana, V. Gonzalez, E. Higon, C. Iglesias, J. M. Lopez Amengual, J. Poveda, B. Salvachua, E. Sanchis, J. Torres, J. A. Valls
IFIC, Centro Mixto Universidad de Valencia-CSIC, E46100 Burjassot, Valencia, Spain

H. Hakobyan, M. Simonyan
Yerevan Physics Institute, Yerevan, Armenia

1. Introduction

The ATLAS Tile Calorimeter (TileCal), in conjunction with the Liquid Argon Calorimeters, provides essentially full absorption of the energy of jets for pseudorapidities $|\eta| < 4.9$. TileCal is divided into three cylindrical structures, extending altogether over the interval $0 < |\eta| < 1.7$. The design of this system is described in detail in the “ATLAS Tile Calorimeter Technical Design Report” [1]. An overall view of the calorimetric system of ATLAS is given in Fig. 1, which also shows the central and the two external cylinders of TileCal, which are referred to as the Barrel and Extended Barrels respectively.

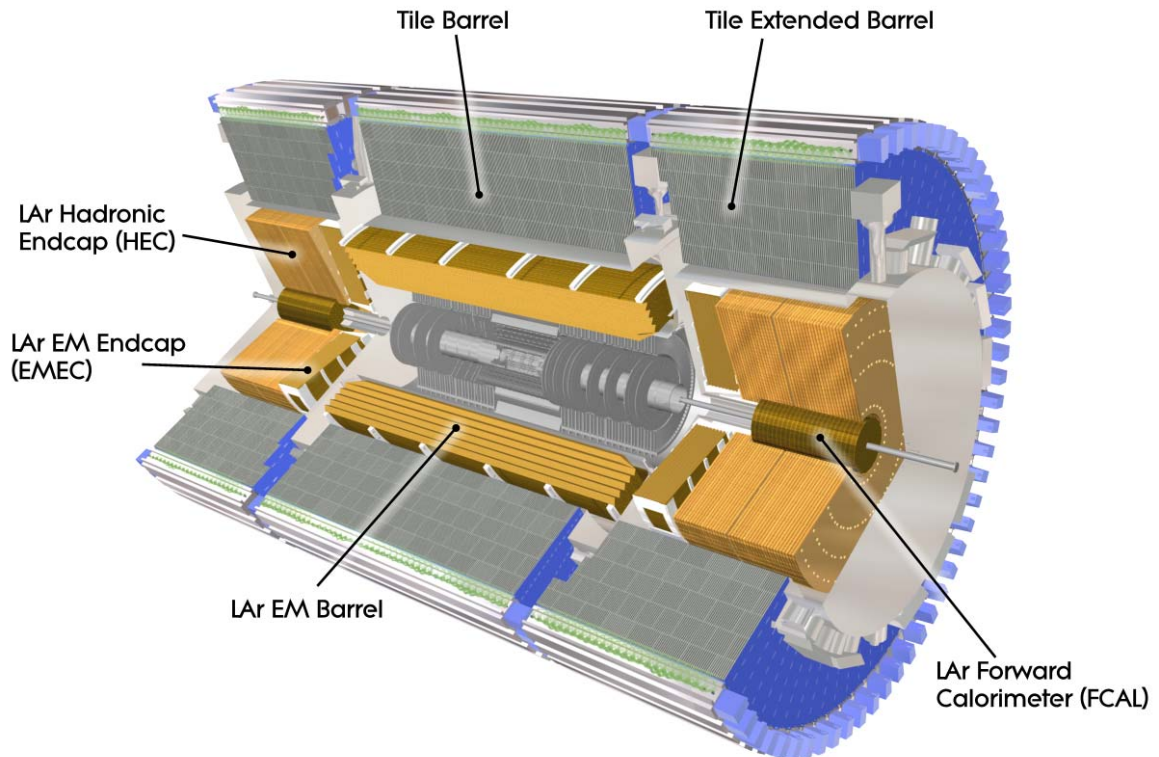


Fig. 1: The Calorimetric system of the ATLAS experiment at the CERN Large Hadron Collider.

Each of the three Barrels is segmented in azimuth into 64 modules, which were constructed and tested in separate production lines. Module construction consisted of two main phases: the mechanical assembly of the steel absorber structure of each module, and the assembly into this structure of the active optical components – scintillators and fibers - that detect the particles produced in the hadronic showers. The purpose of this Note is to describe the optical assembly procedure – called here Optical Instrumentation – and the quality tests conducted on the assembled units.

Altogether, 65 Barrel (or LB) modules were constructed – including one spare – together with 129 Extended Barrel (EB) modules (including one spare). The LB modules were mechanically assembled at JINR (Dubna, Russia) and transported to CERN, where the optical instrumentation was performed with personnel contributed by several Institutes.. The modules composing one of the two Extended Barrels (known as EBA) were mechanically assembled in the USA, and instrumented in two US locations (ANL, U. of Michigan), while the modules of the other Extended barrel (EBC) were assembled in Spain and instrumented at IFAE (Barcelona). Each of the EB modules includes a subassembly known as ITC that contributes to the hermeticity of the calorimeter; all ITCs were assembled at UTA (Texas), and mounted onto

the module mechanical structures at the EB mechanical assembly locations. A detailed description of module construction is given in Ref. [2].

2. General features of the optical instrumentation.

The layout of the TileCal cells in the Barrel and Extended Barrel, together with the properties of the optical components used in equipping the modules are crucial factors in determining the instrumentation procedures and the quality obtained. Therefore these aspects are briefly recalled in this section.

2.1. Cell segmentation.

Scintillator tiles are organized in 11 tile rows of different sizes. The scintillation light generated in tiles is collected at the exposed edges of each tile by wave-length shifting (WLS) fibers, arranged in pre-shaped opaque plastic “profiles”. Within each module, readout cells are defined by grouping together bundles of fibers which are then coupled to a photo multiplier (PMT). Each fiber bundle thus brings to a PMT the light from a group of tiles that spans part of the longitudinal and transverse extent of hadronic showers. The light from each cell is read out by two PMTs, which detect the light from the two exposed sides of each module.

The segmentation of the LB and EB modules into four types of cells/sub-cells – A,B, C and D, from inner to outer radius - is shown in Figures 2 and 3, from Ref. [3]. In the Barrel, the B and C sub-cells are read out by the same PMT.

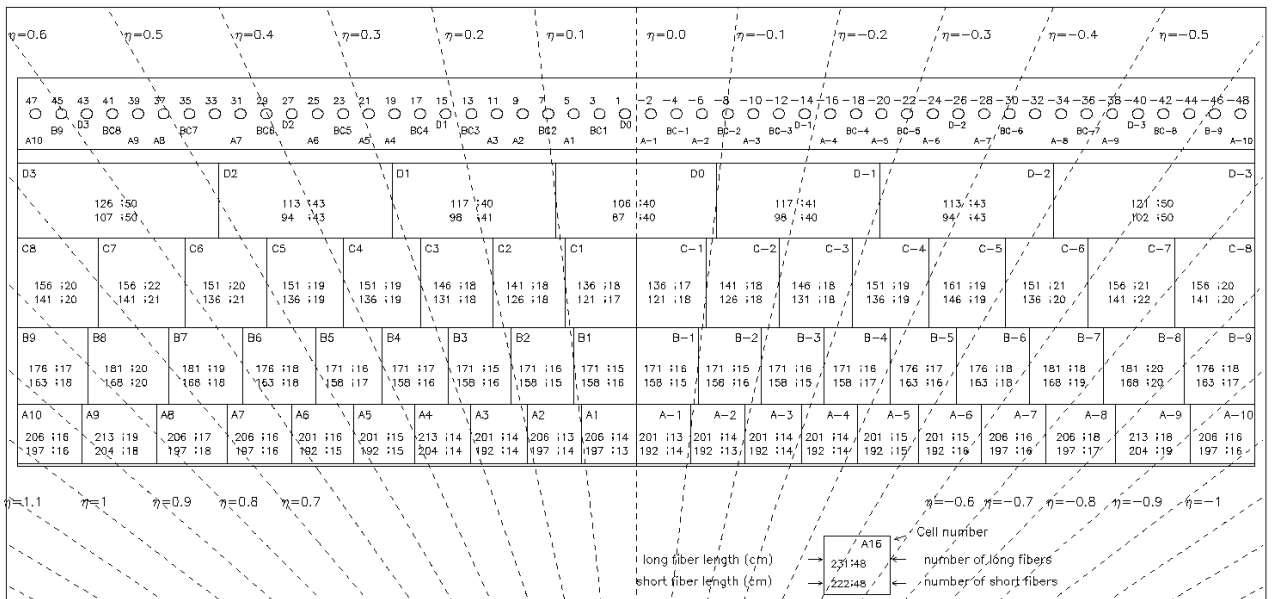


Fig. 2. Layout of cells in the Barrel (LB) modules. The bottom of the picture corresponds to the inner radius. For each cell, the *long* and *short* fiber lengths are given, in cm, together with the number of fibers of each type. For each cell, the number of the PMT that reads it out is also given.

Cells of type A and B are numbered according to pseudorapidity – for instance, cell B-4 covers the interval $-0.4 < \eta < -0.3$ – while D-type cells cover a pseudorapidity interval of 0.2, and are numbered sequentially from the center (*i.e.*, D0 covers the interval $-0.1 < \eta < 0.1$). The Figures

also specify the length (in cm) of the fibers of the two groups within each cell, and their number¹.

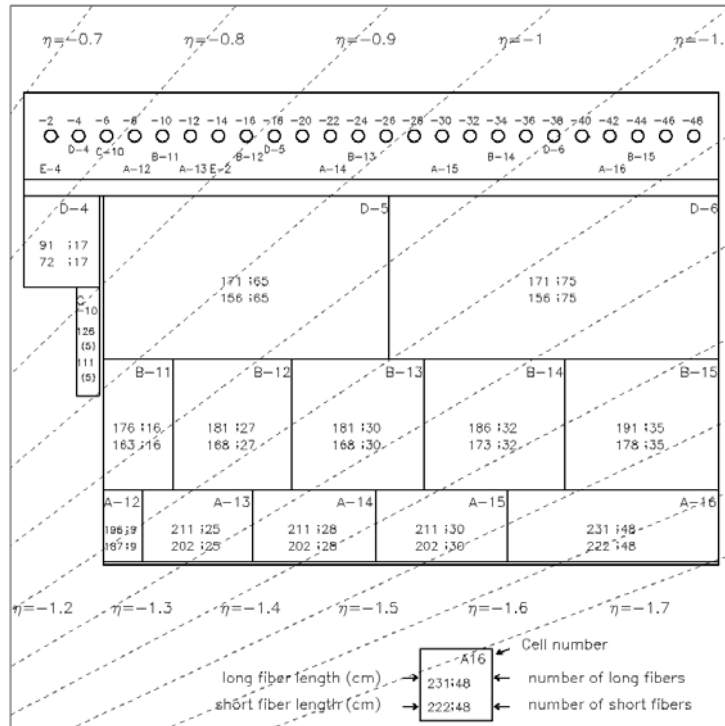


Fig. 3. Layout of cells in the Barrel (LB) modules. The bottom of the picture corresponds to the inner radius. Long and short fiber lengths, and number of fibers in each cell are given, as for the Barrel modules.

2.2 Scintillating tiles.

The scintillator tiles used for the Tile Calorimeter were produced in a Russian company under the supervision of the IHEP-Protvino group. The aspects that turned out to be most important for module instrumentation are summarized here; full details are given in Ref. [4].

In order to keep the instrumentation lines supplied with tiles of all sizes, the scintillators were fabricated in four separate production runs, or “batches”. The initially acquired polystyrene, known as PSM115, was used to produce approximately one-half of the total of about 460,000 tiles. A second type of polystyrene, BASF165H, was used for the second half, because the first type of material became unavailable. The properties of the two types of polystyrene turned out to be significantly different, as described in what follows.

It is worth to describe the aspects of production process that turned out to be important in the optical instrumentation process.

Batch 1 (about 25% of the total amount) is evenly spread over the 11 types of tiles, while batch 2 is made only of tiles 1, 2 and 3, used for the A cells. This allowed equipping about 95% of the modules with the same type polystyrene in the first compartment, which is where the hadronic energy density is highest. Batch 3, about 20% of the total, used PSM115 polystyrene

¹ Within each cell there are two groups of fibers of different lengths: the *long* fibers that read out the tile row at the smallest radius and the next-to-next tile row, and the *short* fibers that read out the remaining tile rows. Fibers of different cells have different lengths, chosen to minimize fiber length and thereby maximize light output, and to reach PMTs with the fewest bends, which optimizes light collection and favors its behavior over time. See [3].

for tile sizes 4, 5 and 6 and BASF165H for sizes 7 to 11. Finally, batch 4 is entirely made with BASF165H material,

The most important characteristics of the scintillating tiles are light yield and transmission. These properties were monitored during tile production by measuring two parameters, I_0 and I_1 , proportional to the current in a PMT that reads out a WLS fiber coupled to one of the two short edges of a sample tile. The I_0 signal was produced by a radioactive source placed on the tile next to the readout fiber, while I_1 was obtained placing the source near the far edge of the tile. I_0 is a rough measurement of light yield, while the ratio I_0/I_1 is a sensitive figure of merit related to the transmission of light over the width of the tile, because smaller I_0/I_1 corresponds to better transmission. On the production line, I_0 and I_1 were measured on one out of every 20 tiles, and the values of I_0 and I_0/I_1 were recorded for every pack of 20 tiles containing the one thus measured.

The average values of I_0 and I_0/I_1 for the four production batches and for the tile sizes produced in each batch are given in Fig. 4. It is clearly seen that the tiles made with BASF 165H polystyrene have a significantly higher light yield, because all tile sizes of batch 4 display a higher I_0 value. However the transmission of the tiles made out of this material is only slightly better than of those made of PSM115, as shown by the plots of I_0/I_1 for the different production batches.

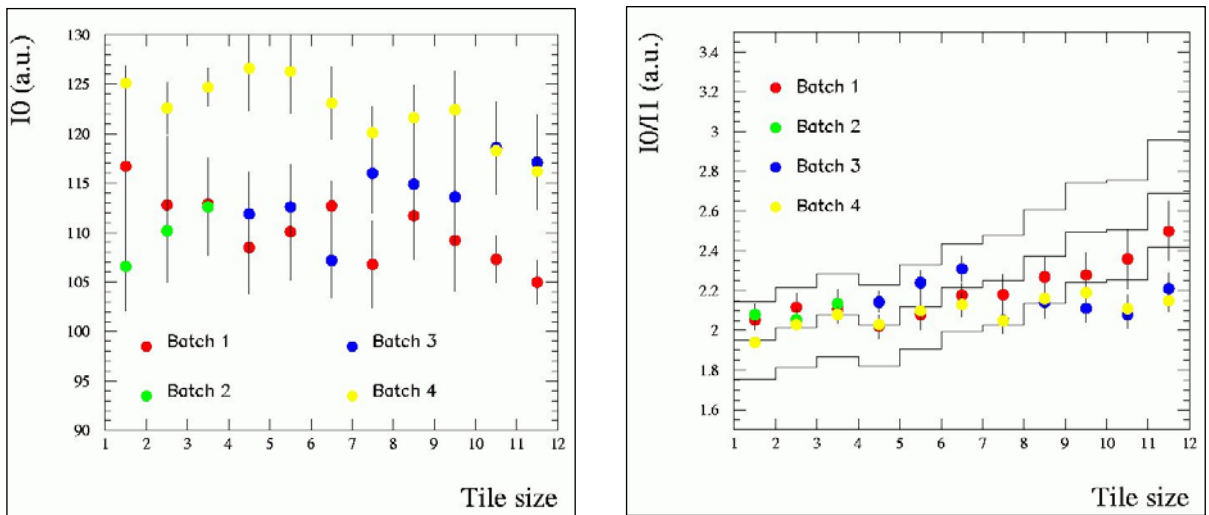
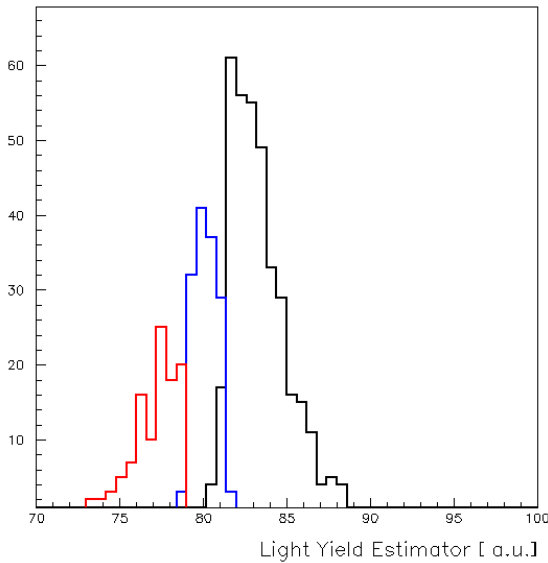


Fig. 4. The average light yield and transmission parameters, and their RMS deviations (error bars) for each tile size and production batch. The three lines in the plot of I_0/I_1 indicate an “acceptance corridor” for the transmission figure of merit as function of tile size, which is better than specified for the larger tile sizes and the later batches (lower I_0/I_1 = better transmission).

The variation in light output of tiles within the same production batch, visible in Fig. 4, made it useful to assign tiles to modules with a procedure designed to improve optical uniformity within modules. From batch 2 onwards, the packs of 20 tiles were ordered according to the quantity $(I_0 \cdot I_1)^{1/2}$, which was shown to be a better estimator of optical quality than I_0 alone. Then the approximately $1/2$ of the tiles with the higher values of $(I_0 \cdot I_1)^{1/2}$ were used for the barrel modules, while the remainder was again divided into two equal samples, ordered by the value of the optical quality parameter. By random extraction the sample with the higher $(I_0 \cdot I_1)^{1/2}$ values was destined to the instrumentation of the EBC modules, and the other to EBA modules. The selection procedure is demonstrated in Fig. 5, where the histograms show the distributions on the light estimator $(I_0 \cdot I_1)^{1/2}$ for packs of tile size 10.



The black histogram corresponds to packs assigned to the barrel module instrumentation, while the blue and red ones denote the packs assigned to EBC and EBA respectively. (The small overlaps are due to the simplified selection procedure that was adopted in this case: as tile packs came in large crates, if most of the packs in a crate belonged to one group, these packs were not sorted but the entire crate was destined to one instrumentation site.)

Fig. 5. Example of the selection procedure in batch 4. See text for details.

Other procedures adopted in the instrumentation laboratories to optimize module uniformity are described in the Appendices.

2.3 WLS fibers

In contrast to the scintillating tiles, the characteristics of the WLS fibers used in module instrumentation were rather uniform across the entire lot.

The general organization of the WLS fiber subproject – involving fiber procurement, QC, aluminization, and the development and production of profile and fiber assemblies – was managed by the LIP and the Pisa groups [5, 6].

The 1 mm diameter Y11(200)MSJ fibers produced by Kuraray were aluminized at the end opposite to the PMTs to increase the light yield and to get better uniformity in the region where they collect light from the scintillators. The RMS deviation of the light output of the aluminized fibers, averaged over a group of fibers of the same length, was found to be about 3%, as can be seen in Fig. 6 (see also ref. [7]). The fiber bundles with an RMS deviation of more than 7% were rejected.

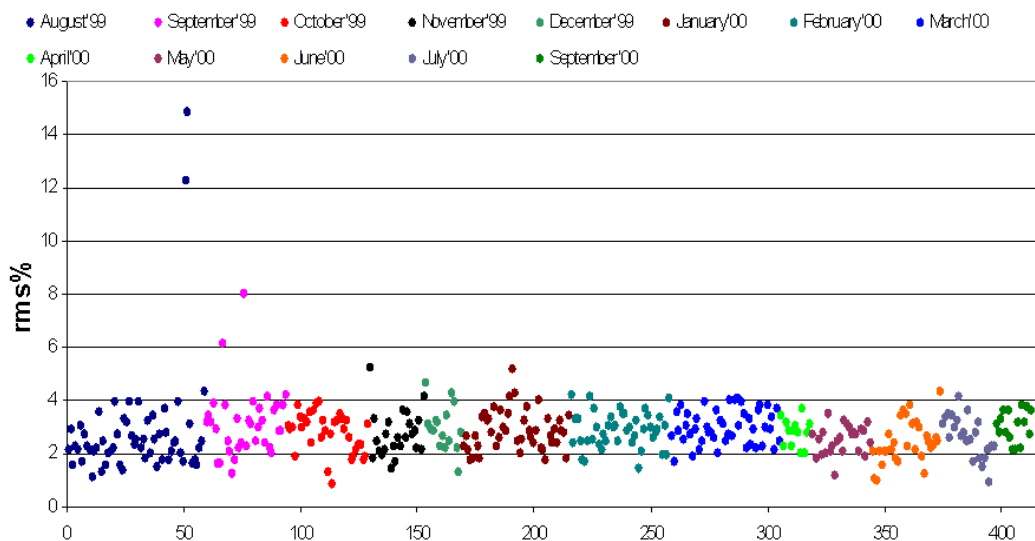


Fig. 5. Results of the quality control of the aluminized fibers. The RMS of the fiber relative light yield for each bundle of fibers is shown. The colors indicate the date of production of each batch.

3. General description of the instrumentation and quality check procedures.

A substantial effort was made to adopt common procedures in all instrumentatins sites. By and large, the sequence of operations was identical; it is schematically described in this section. The main differences are to be found in the tile sorting and masking procedures, which are described in detail in the Appendices.

Instrumentation of a module began by mounting the mechanical structure on an appropriate support. The instrumentation procedure consisted of the following steps:

- Cleaning of the tiles slots and checking the module geometry
- Inserting the tiles, previously wrapped in Tyvek sleeves
- Applying to both sides of the module the plastic profiles containing the optical fibers, using tooling to ensure a proper optical coupling to tiles
- Collecting fibers into bundles, where each bundle contains all fibers belonging to a cell
- Checking the proper fiber contents of the bundles with a calibrated line of LEDs inserted into the source calibration holes.
- Routing the bundles into the available space, and adding to the bundles the test laser fibers
- Potting the individual fiber bundle assemblies into their dedicated Lucite containers, using optical quality epoxy glue
- Cutting and polishing the edges of the fiber assemblies
- Checking the optical quality of the fiber edges with a TV camera moving in the steel girder that constitutes the structural backbone of each module.

This step concluded the basic instrumentation phase and was followed by the procedures to prepare for and execute the quality checks. These differed depending on whether the optical quality was checked by means of a ^{137}Cs radioactive source (as was done at CERN and at ANL) or by an LED (at IFAE and Michigan). In the case of source checks, in each tile row a steel rod and a steel tube were inserted through the length of the module, traversing each tile (the steel rods and tubes hold in place every tile; in addition, the tubes provide the paths for the source). In the case of LED checks, one steel rod and one transparent plastic tube were inserted in each tile row.

The quality check consisted of the following steps:

- Inserting a test drawer with PMTs and readout electronics
- Connecting the low-voltage and high-voltage power, and starting up the local DAQ system to read out the PMTs responses
- Checking the test laser fibers functionality with an LED source
- Running either a Cs^{137} source or an LED through the steel or plastic tubes to record the light signals from each tile and each fiber and check their adequacy
- Making the repairs or replacements of optical components needed to obtain the uniformity specified below
- Repeating the source/LED runs to recheck the obtained performance
- Storing the certification results to a data base

The criteria applied in checking the optical quality of modules and to certify it were the following two:

- All the individual tile/fiber signals (two per tile) deviating from the tile row segment average by more than 25% were diagnosed and followed by corrective action (in most cases, replacement of a fiber or of a tile)

- The module's overall uniformity, defined as the RMS deviation of the mean cell signal from the average of all cells in a module, was required to be better than 10%.

An LB module, partially equipped with WLS fibers, is shown in Fig. 8.

It is worth mentioning that a substantial organizational effort was made to have identical or very similar tooling and procedures at all instrumentation sites. In addition, the sites stayed in close contact with each other. Any improvement in module instrumentation proposed at one of the sites was tested and usually adopted by all other sites within several days. Thus, while uniformity in the instrumentation procedure was preserved across different sites, the instrumentation and certification techniques converged to their final state rather rapidly, within a few months from the beginning of the instrumentation campaign.

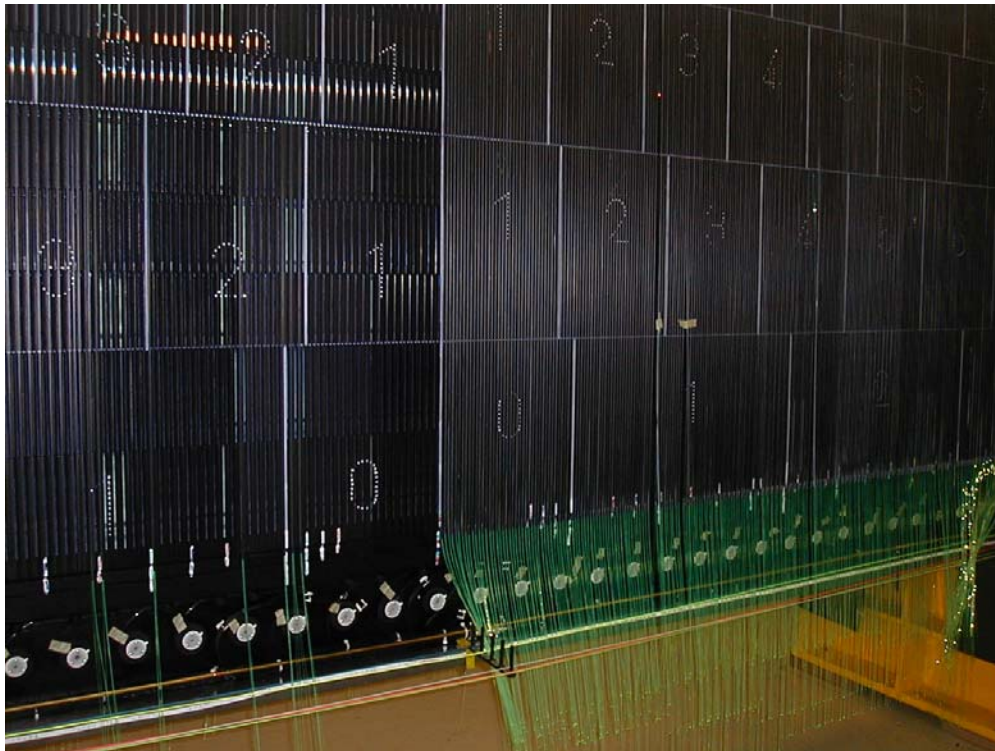


Fig. 8. An LB module partially instrumented. The numbers and the white line indicate the cell boundaries and the median plane of the module. All the tiles are inserted, but only part of the WLS fibers are in place, on the right of the median plane (continuous vertical line). The fibers from different radial segments (A, B, D) are kept separate by colored strings.

4. Procedures and quality checks at the instrumentation sites

4.1 CERN instrumentation Site

LB modules mechanically assembled at JINR (Dubna) were delivered to CERN beginning in August 1999. The instrumentation facility was set up at Bldg. 867 on the CERN Preveessin site, in space conditioned to support a clean working environment. Up to four LB modules could be placed in the room at one time. In Fig. 8 the very first LB modules (JINR#01, JINR#02, JINR#03 and JINR#04) are shown; they are at different stages of optical instrumentation.

The equipment for module quality checks was located outside the instrumentation room. Its main component was the hardware and the electronics of the hydraulically driven Cs¹³⁷ source system.



Fig. 8. The instrumentation room at the CERN Preveessin site. Four Barrel modules are at various stages of instrumentation, from tiles and fiber insertion to fiber routing and repairing. Calibration tubes to check the optical quality of with the ¹³⁷Cs source are seen on the front end-plates.

All 65 LB modules were instrumented and certified in three years, from August 1999 to September 2002. The detailed logbooks of the LB module instrumentation, including the quality controls, repairs and final certifications are on record in the following web page:

http://atlas.web.cern.ch/Atlas/SUB_DETECTORS/TILE/production/optics/instrumentation/monitor/cernproduction.html

Several steps of LB modules instrumentation at CERN are shown in Figures 9, 10 and 11.



Fig. 9. Inserting tiles and profiles with fibers into a Barrel module

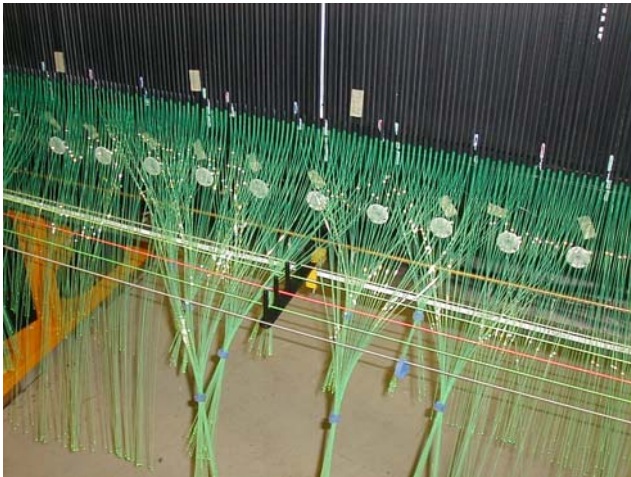


Fig. 10. Sorting of fibers into bundles ((left); fiber bundle routing (right)

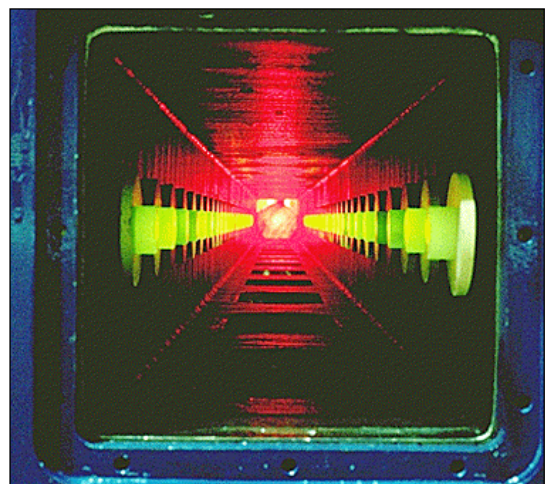
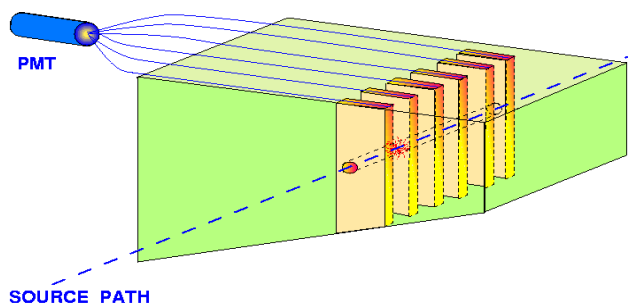


Fig. 11. A fiber bundle ready for being potted into a Lucite container (left). Bundles inside the module girder after cutting and polishing the surfaces facing the PMTs (right)

The quality checks of the instrumented modules are described next. All modules were scanned with a prototype of the TileCal ^{137}Cs γ -source system, developed from 1996 onwards at the SPS test beam and certified to become the main calibration and monitoring system for the entire TileCal in the ATLAS cavern.

A detailed description of the system design and performance can be found elsewhere [8, 9]. Only a few aspects of the source system, relevant to the module quality checks, are reviewed here.



The source scan scheme is shown in Fig. 12. A capsule containing a ^{137}Cs source of a few mCi, is hydraulically driven through a system of steel tubes that traverses every scintillating tile in a module. The 0.662 MeV γ -rays emitted by the source produce light in the scintillator and a current signal in the PMTs that read out the cell traversed by the source. The signal clearly displays the tile structure of the module, as seen in Fig. 13.

Fig. 12. The concept of the Cs^{137} source scans.

This is due to the fact that the mean-free-path of the γ -rays in the calorimeter structure is about equal to the 18 mm calorimeter periodicity. Due to this feature faults at the location of any tile is visible. In the figure, it can be seen that the signal from a tile in cell B+2 is strongly suppressed; in this particular case, a WLS fiber coupled to this tile is at fault.

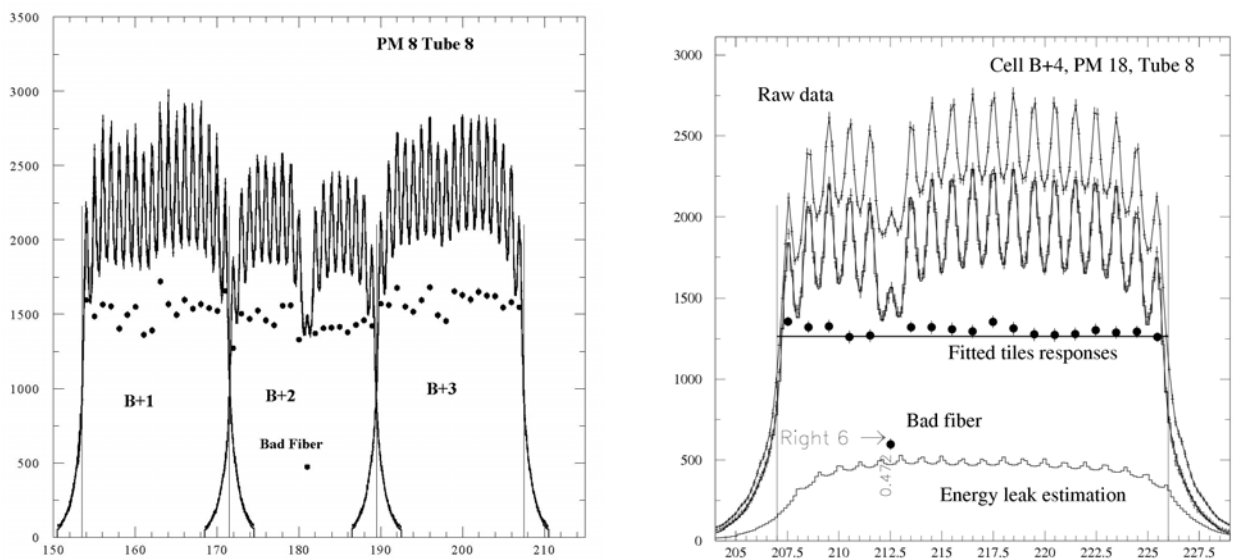


Fig. 13. Left: A source scan, showing a faulty fiber. Right: another source scan, in which the strength of the fitted tile responses is shown. The upper plot is the raw signal, which is the sum of the signal from the tile row through which the source has passed (middle plot) and of the signal from the tile row adjacent to the tube in which the source passed (lower plot).

Thus source scans provide a powerful means to diagnose optical instrumentation defects, but also to measure the response of each tile-fiber channel. This is shown in Fig. 11 (right panel). The contribution to the signal of each tile is deconvoluted from the sum signal by fitting the

sum with a model shape for the tile signal. The individual tile signal is obtained with an estimated precision of 2%.

The data shown in Fig. 11 were displayed on line during module quality checks, which allowed making immediate decisions about repairs to the optical components. The typical faults are due to a bad or broken WLS fiber, a faulty tile-fiber coupling, or a poor scintillator.

The basic criterion was to inspect and repair any instance of a “tile peak” with less than 75% of the mean value of the tile row belonging to the cell being scanned. The reason of this quality cut is as follows. What matters is the average response of a cell (typically composed of 2 or 3 tile rows, and >30 tiles) – therefore the requirement on the uniformity of response of any tile-fiber subchannel can be set rather loosely, because even a 50% loss of signal as in the figure will lead to a <1% loss of signal on the entire cell. It can be seen that the 75% criterion a conservative choice.

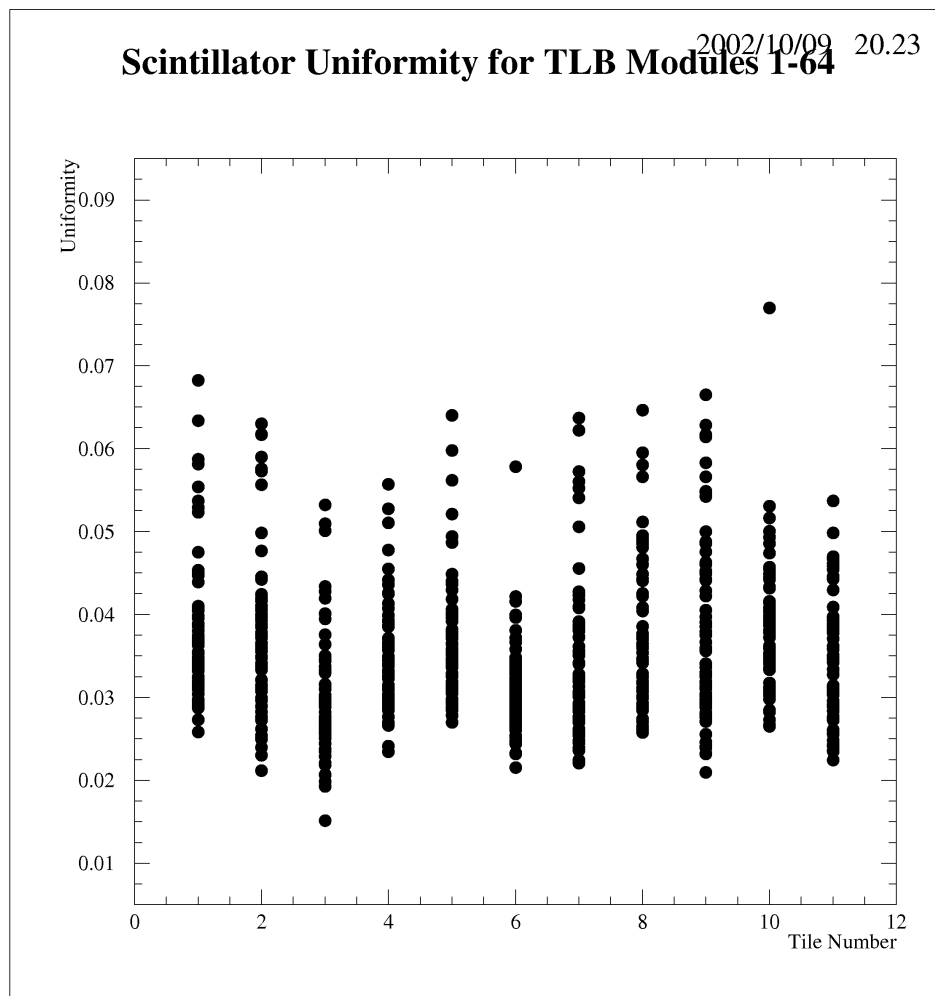


Fig. 14. The RMS of the individual tile signals over each of the 11 tile rows.

The uniformity over each tile row of the 64 production barrel modules is shown in Fig.14. Each point is the RMS deviation from the mean of the individual tile signals, taken over each tile row, for each module. Thus every point gives an RMS value taken over 307 tiles. This uniformity does not depend significantly on the tile type and is distributed over a range of 2% to about 6% for all modules, with typical values of 2% to 4%. It is understood to be the result of a combination of the variation of tile response and of fiber optical fiber coupling efficiency within each tile row.

4.2 IFAE-Barcelona instrumentation site

Instrumentation of the Tilecal EBC modules began at IFAE-Barcelona in October 1999. Sixty four extended barrel modules mechanically assembled in Spain with the participation of the Valencia and Barcelona groups were optically instrumented, certified with a light source, and all shipped to CERN by March 2002 where they were eventually assembled in the EBC barrel of the Tile calorimeter.

The instrumentation and initial certification of EBC modules took place in the IFAE ATLAS workshop using dedicated tooling that included a 16-ton crane, a fiber routing mockup, a movable structure that produced dark room conditions, and various custom-made gadgets for quality certification. This equipment was distributed between two workshop areas permitting work to be conducted on two modules independently, as illustrated in Fig.15. On average, it took two working weeks to complete an instrumentation cycle on a given EBC module with work taking place on two modules in parallel.

As EBC modules were produced, instrumented and delivered to CERN they were assigned a sequential number from IFA01 to IFA64. This numbering corresponds to the order in which modules were instrumented. Since the instrumentation and certification procedures evolved during the instrumentation campaign, some of the optical properties of the Tile modules display a dependence on the order in which they were instrumented, as shown below.

As pointed out in Section 3, improvements in the instrumentation procedure were rapidly communicated from site to site and were usually adopted within days in all sites. An example is given here. Early in the campaign a method was found to insert additional fibers into a bundle when a few of the already potted ones were found to be defective. One or a few Teflon tubes were added to the WLS fiber bundles when potting them into their Lucite tubes. The Teflon tube was then extracted and the hole thus produced was used later to introduce a new WLS fiber.

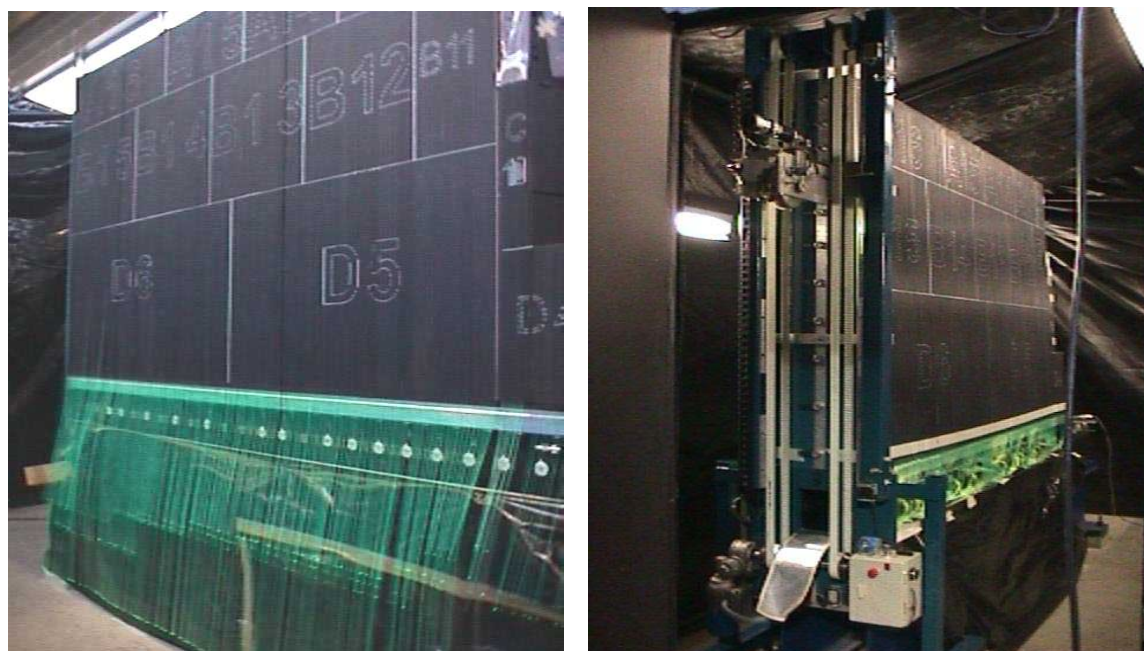


Fig. 15. Two instrumentation areas at the IFAE-Barcelona workshop. On the left, module IFA08 is being instrumented. On the right, module IFA07 is placed in a dark room and is being certified with the movable LED light source system.

A picture of a polished fiber bundle can be seen in Fig. 16. This technique replaced fiber splicing, which was used earlier to repair broken WLS fibers; it was implemented on all TileCal modules instrumented after IFA05.

The module certification procedure applied at IFAE is described next. The method was based on measuring the signal generated by producing blue light within each tile. The light was generated by a NICHIA NSPB-310A, with an emission spectrum from 440 nm to 550nm, closely resembling that of TileCal scintillators (450 to 490 nm). The blue LED light was transmitted through each tile, absorbed by the WLS fibers and re-emitted as in the case of scintillation light.

The LED was potted with light-diffusing epoxy into a transparent plastic tube, in order to make the source azimuthally symmetric. The assembly was encapsulated in an aluminum tube, with a 3 mm wide transparent window. The components of the light source are shown in Fig.17. The LED was set to operate in continuous mode with a dedicated current source. The azimuthal non-uniformity of the light source was measured to be less than 2%. The light source signal as measured by the TileCal module PMTs had an RMS deviation over a few days of less than 1.5%, which includes variations of PMT gains.

The light source was inserted through transparent plastic tubes which traversed each of the eleven tile rows, passing through the holes destined to final certification with the ^{137}Cs radioactive source. The light source was driven by a dedicated electro-mechanical device designed and built at IFAE, which is shown in Fig. 18. The device was programmed to move the light source vertically to the point of insertion into each tile row, and then to insert it, advance it through all tiles, retract it and repeat the cycle for all tile rows. The source velocity was stable at the level of 0.3%. The PMT signal was read out by the TileCal integrators used for ^{137}Cs and minimum-bias signal readout. The response was measured twice per millimeter, at a rate of 75 Hz; a full scan of a module took twenty two minutes.



Fig. 16. Screen from a mini camera showing a polished Lucite tube with bundle of bright WLS fibers and dimmer points from two Teflon tubes, used to insert spare fibers if needed, at the edge of the bundle at about 4 hours.

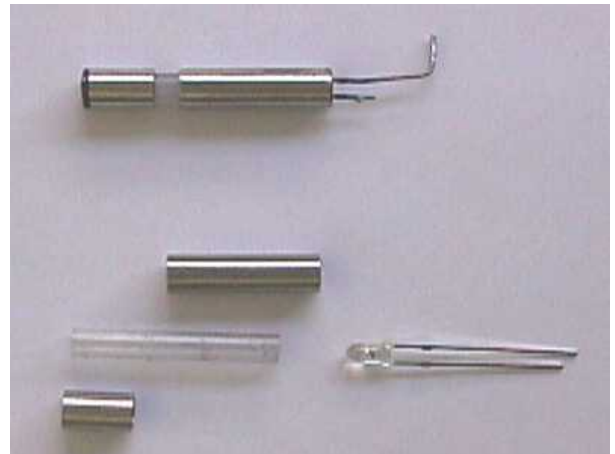


Fig. 17. LED-based light source used to certify the quality of the instrumentation at IFAE. Shown are the LED, the transparent plastic tube, the Al tubes and the final assembly, with an azimuthally symmetric 3 mm window.

The movement of the source, the LED and PMT power supplies data acquisition and display, as well as on-line quality checks and data storage were controlled with a program based on LabView5.0 but incorporating C++ code. The graphic interface is shown in Fig. 19.

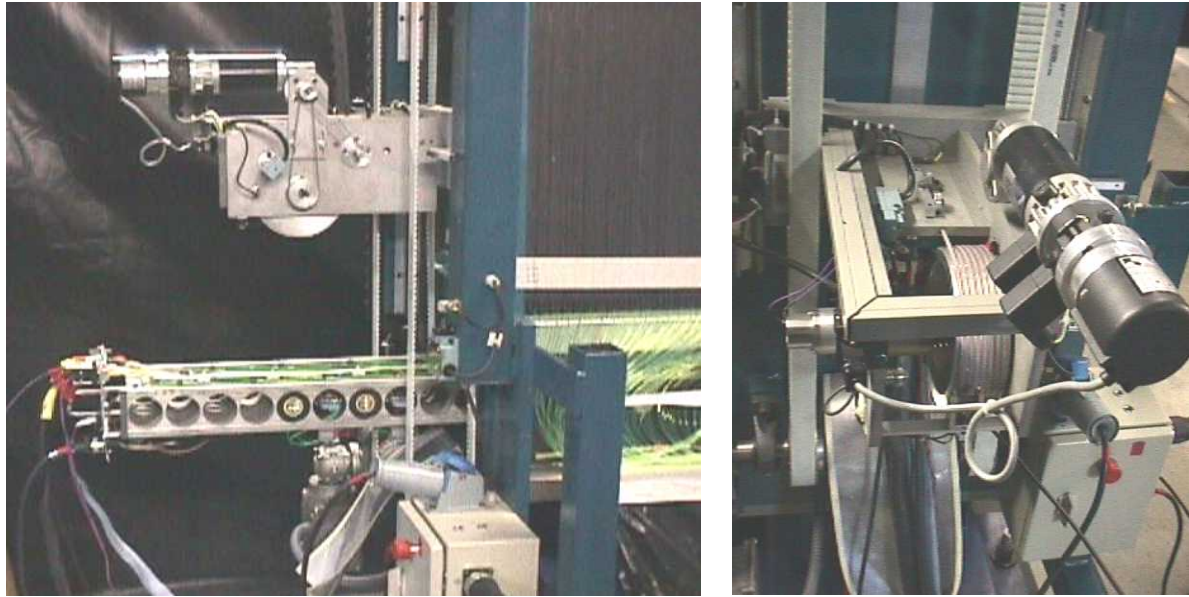


Fig. 18 The device that guided the LED light source through tiles for module certification.

Immediately after data-taking an analysis package was run on the raw data. The passage of the LED through each tile generated a characteristic triangular signal, as shown in Fig. 19. The combined tile/fiber response is proportional to the integral of this signal. The repeatability of the absolute (relative) measurement of this response was found to be 1.5% (0.6%) over several days and was limited by the combined stability of the light source and the PMT gains in the environment with no temperature control. Comparison of a given tile/fiber response to other responses within the same module, specifically to those belonging to the other side of same tile and to other tiles read out by the same fiber, allowed an automatic diagnosis of the most likely location of most optical faults. An example of a program-detected fault is shown in Fig. 20.

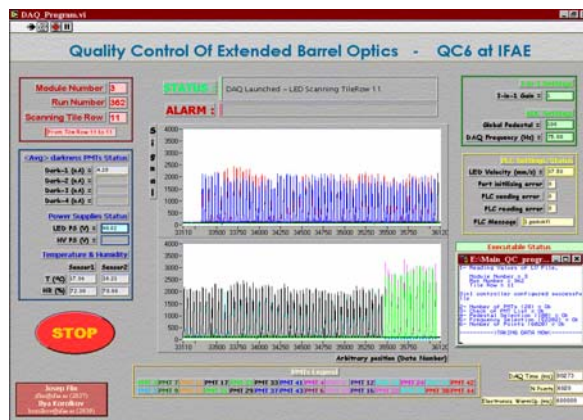


Fig. 19. Graphic interface of the DAQ program described in the text. The signals from 145 tiles of module IFAE03 are displayed; different colors correspond to different readout channels.

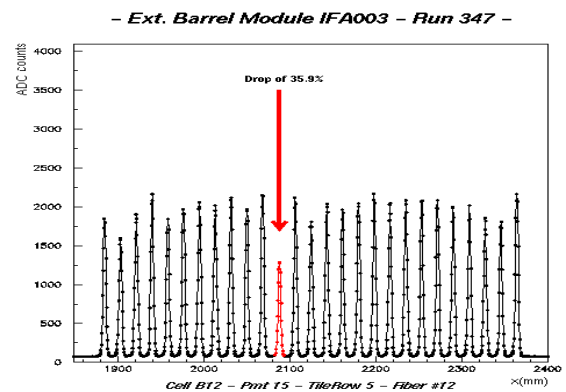


Fig. 20. An example of an automatically detected and later repaired fault in a single optical coupling, observed in module IFA03.

The threshold to investigate and possibly repair an optical fault reported by the data analysis package was initially set at a deviation of 30% from the average of the tile/fiber responses in a module. This threshold applied to modules IFA01 to IFA14. In agreement with the other instrumentation sites, the threshold was tightened to 25% from IFA15. Typically, out of a total of 3182 tile/fiber responses per EBC module, 10 to 30 cases were found where this threshold was exceeded in the first module scan. An example of a summary report automatically

generated on raw data by the analysis package, just after completing instrumentation, is shown in Fig. 21.

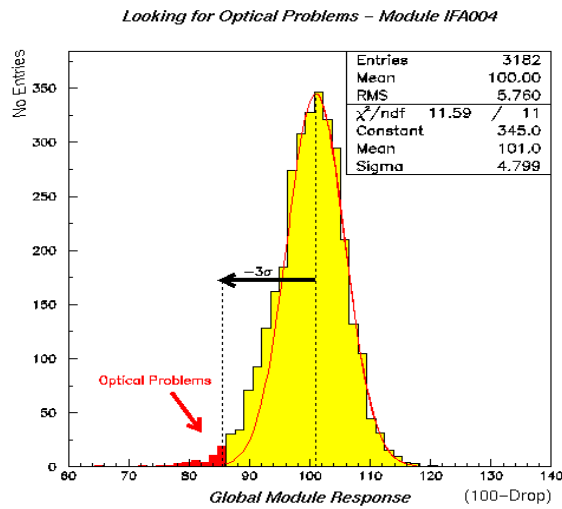


Fig. 21. Distribution of the tile/fiber responses normalized to their average for module IFA04. The Gaussian fit of the distribution and the low-response tail beyond 3σ are shown in red.

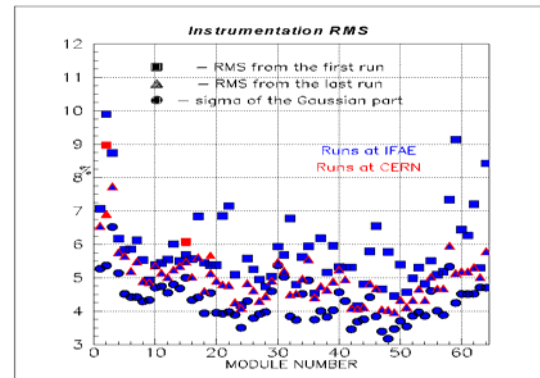


Fig. 22. The spreads in the tile/fiber responses of all 64 EBC modules instrumented at IFAE vs. module sequential number. The RMS values before (after) repairs at IFAE are represented by blue squares (triangles). Circles indicate the Gaussian σ of the distributions.

Statistical analysis of all failures observed during the instrumentation of EBC modules showed that about 70% of abnormal optical responses were due to inadequate tile-to-fiber couplings that included: profiles not well introduced in the slot between the master plates, fibers stuck between iron and scintillator, and fibers not well centered. It was noted during the instrumentation that the width of the Gaussian part of the optical quality distribution, as shown in Fig. 21, was almost entirely determined by the quality of the tooling used during the fiber profile insertion. About 25% of abnormal optical responses were due to fibers. Among them were fibers not reaching the bundle end or fibers that did not cover the entire readout end of a tile, damaged fibers, fiber routing errors, and fiber ends not adequately polished. The final 5% of the abnormal optical responses were due to problematic scintillator tiles: abnormal tile transparency, a displaced Tyvek envelope, or chipped tiles. Most of these faults were repaired during several sequential attempts leaving on average only 0.7 cases per module without a successful repair. The majority of the relatively low response cases that remained in the EBC modules are due to the limitations of the fiber splicing technique that was rendered obsolete from module IFA05 onwards by the additional fibers that could be installed in the holes created with Teflon tubes, as already described.

The spread of tile/fiber responses measured on each module before sending it to CERN is a useful summary of the optical quality of the modules; it is shown in Fig. 22.

Measurements of tile/fiber responses made by LED and the Cs sources, after module delivery to CERN, correlate at a 90% level, indicating that the variation in tile light yield, to which the LED source was insensitive, gave only a minor contribution to the non-uniformity of the Tile module response across its volume. A significant, if variable, fraction the time spent on each module went to quality checks, repairs, and certification. As a result, the optical quality of the instrumented EBC modules was kept under close control and significantly improved with module sequential number.

4.3 Instrumentation sites in the USA

The mechanical structure of the extended barrel modules EBA was prepared at Argonne. Half the modules were instrumented at Michigan State University, MSU, and half at Argonne, ANL. Final QC at MSU was done by using an LED source, and at ANL it was done by using a Cs137 source. Examples of the resulting plots are shown in figures 23,,24, 25, and 26.

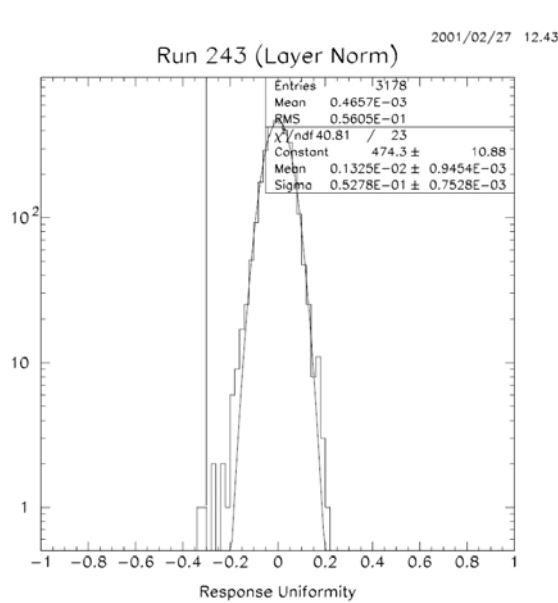


Fig. 23. Distribution of the tile/fiber responses measured with a Cs137 source and normalized to their average for module ANL-24 which was instrumented at Argonne. The Gaussian fit of the distribution and the low-response tail beyond 3σ are shown.

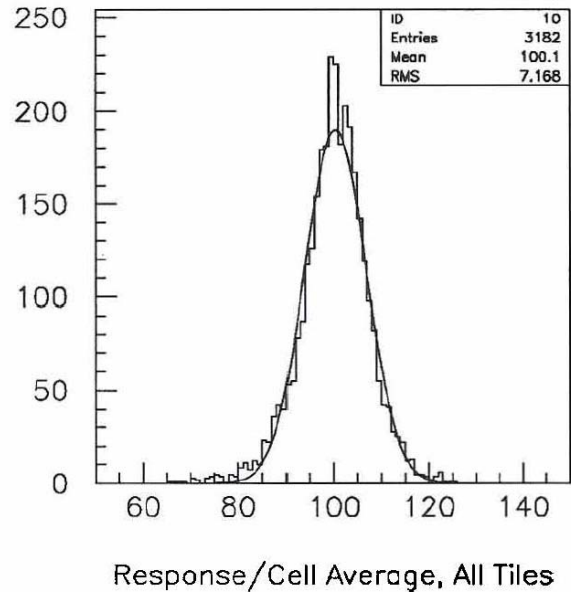


Fig. 24. Distribution of the tile/fiber responses normalized to their average for module ANL-09 instrumented at Michigan State and measured with an LED light source. The Gaussian fit of the distribution is shown.

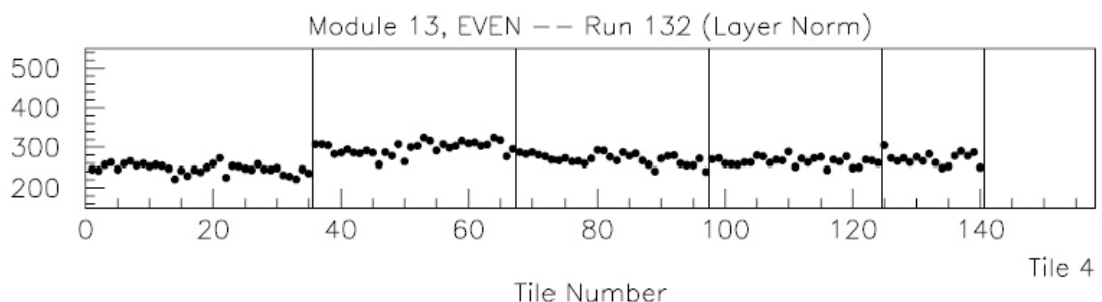


Fig. 25. An example of a Cs scan done at ANL. This one is for tile row 4, looking at the side with even number PMTs.

The web was used for keeping track of Quality control measurements during the entire production of the EBA modules.

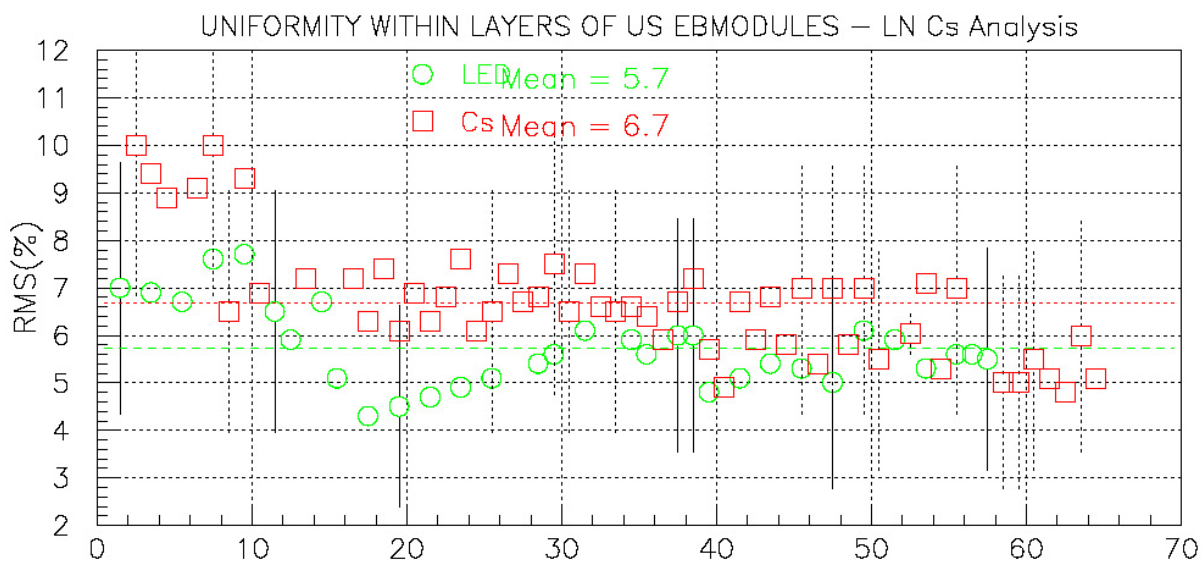


Fig. 26. This graph from one of the QC webpages shows the uniformity of response within layers over all 64 EBA modules as measured with the Cs137 source at Argonne. There are similar plots of uniformity within cells, and also uniformity of tiles and fibers.

Cs scans were done at ANL for all EBA modules, both those instrumented at ANL and those instrumented at MSU. There are databases on the web for these scans at Argonne HEP. Also, the QC logbook for each module is saved at Argonne. These logbooks contain a record of the scans which were done and the repairs which were made to meet the quality criteria. The electronics drawer for these scans was set up as follows: For the first module, the High Voltages to the Phototubes were adjusted so that all the peaks were roughly the same amplitude. These High voltages were then stored in the control microprocessor and never changed again. This allowed consistent checks over the history of the construction project. A picture of the source driver is shown in figure 34. The source illuminated one tile at a time strongly, and adjacent tiles weakly. The same was true of the LED source at MSU, shown in figure 28.

There were extensive checklists used, seven pages for the mechanical assembly, and nine pages for the instrumentation. An example page is shown in figure 30. Many procedures were developed in order to control the quality of the mechanical structure. We give one example. The sub modules of ten iron plates and 10 layers of spacers were aligned on the girder with angular and spatial tolerances to permit assembly of the final modules into a circle in ATLAS. There were bars welded at the inner radius to preserve this alignment and strengthen the module. Due to variations in the thickness of steel plates and glue viscosity, there were very small variations in the thickness of the sub modules. In some cases, thin shims of size roughly 2 meters by 5 cm by 0.5 mm were used to insure that the tiles and fiber profiles fit for maximum optical coupling and stability.



Fig. 27 Various profile insertion tools were developed at ANL as well as at the other sites. This ANL tool compresses the fiber profile, and directs the compressed part into the slot between steel plates at the tile edge.



Fig. 28 This LED light source was used for the QC measurements at MSU. It was guided through the holes in the structure which would normally accommodate the source tubes. The LED could then illuminate each tile individually.

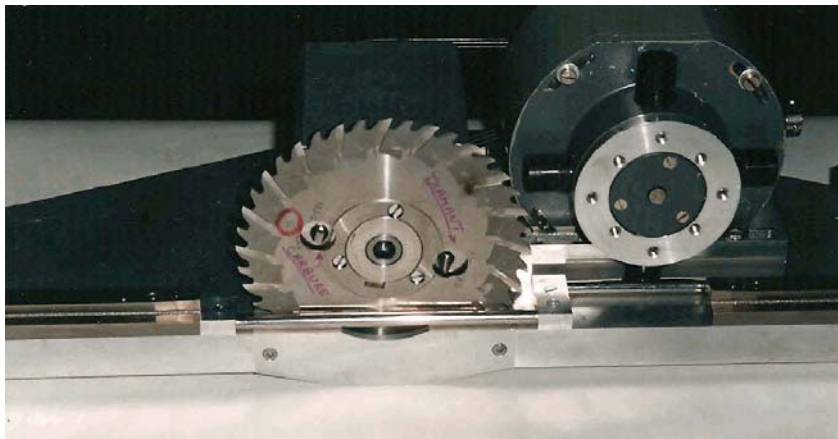


Fig. 29. The same type of cutter for the aspirin tubes was used at all three sites. One can see the saw for the initial cut, the carbide cutter for the slightly closer cut, and the diamond cutter for the final cut to achieve optical quality.

- **Aspirin Tube Installation:**

IMPORTANT: Do not remove cleaned sets of Aspirin Tubes from their storage bags before holes are reamed and cleaned (Step 8 below)!

Following steps must be done in sequence.

24.07 ADJ. REAMER
24.06 - 24.08 GOAL

1. Ream Girder Rings for Aspirin Tube slip fit (24.10 mm reamer provided - size checked). Do not ream unused Girder Rings except holes # 25, 26, 48, & 49!

Fig. 30. A fragment of the checklists used during construction. The Mechanical Preparation Checklist had 7 pages, and the Instrumentation checklist consisted of 9 pages.

Module Fabrication Checklists Topics:

- A) Clean the Girder.
- B) Install Girder rings.
- 1) Start Module QC file
- 2) Place girder on assembly base. Align in phi and Z.
- 3) Align transit with girder centerline. Put down external references and track string.
- 4) Select and stage sub-modules next to girder. Inspect IR and OR welds. Check all threads.
- 5) Collect all sub-module QC sheets for Module QC file.
- 6) Place submodules on the girder. Align in phi and Z.
- 7) Check that all bolts are torqued the correct amount.
- 8) Measure phi alignment and record in QC sheet.
- 9) Mount endplate on girder. Check phi and Z alignment.
- 10) Weld in front plate.
- 11) Certify the front plate weld.
- 12) Check endplate phi alignment. Then pin endplate.
- 13) Measure overall phi alignment with 8 ft long straight edge, record on QC sheet. (Typically within 0.003 inch at girder, 0.010 in. at top, 0.010 in using plumb bob.)
- 14) Measure and record Module length.
- 15) Inspect all profile grooves and slots. Clean as needed. Touch up paint.
- 16) Paint endplate and front plate blue. Paint girder edges black.
- 17) Stencil module with it's number.
- 18) Check that position B,C,D sub-module bolts are torqued to 250 N/M.

Preparation for Instrumentation Topics:

- 1) Check Scintillator and Profile slot widths. Clean as needed.
- 2) Drill holes for brackets, covers, laser fibers.
- 3) Tap holes for Girder rail studs, ITC fiber holder brackets.
- 4) Clean the rods.
- 5) Check source tube holes and rod holes.
- 6) Remove debris with an air hose.
- 7) Stencil boundaries and profile cells.
- 8) Make strap bracket. Install brass rail and strap brackets.
- 9) Measure for shims. Install shims.
- 10) Check edges of installed shims.

Instrumentation Checklist Topics:

- 1) Prepare module. (Cleaning, Aluminum tape, Vinyl tape.)
- 2) Prepare for Aspirin tube insertion.
- 3) Aspirin tube installation, including reaming.
- 4) Tile Insertion checklist.
- 5) Profile Insertion checklist
- 6) Fiber routing checklist (separate on even and odd sides)
- 7) Aspirin tube stuffing checklist
- 8) Gluing checklist.
- 9) Cs scan
- 10) List fibers/tiles with response less than 72% of nominal

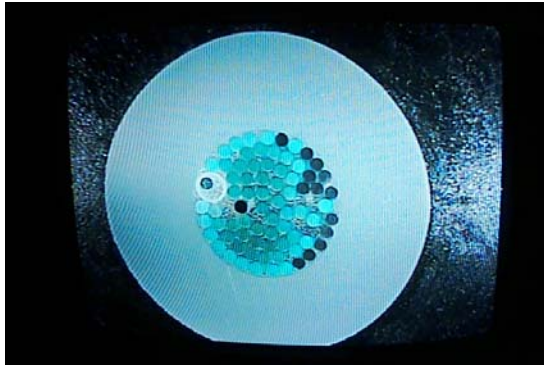


Fig. 31. In this view of a cut and polished aspirin tube one can see the fibers, teflon tubes for extra fibers, and the larger channel for injecting the epoxy.



Fig. 32. A variety of techniques were used to hold the fibers within the allowed envelope. The cloth tape is visible in this picture.



Fig. 33. A view of the inside of the Girder during the cutting and polishing process.



Fig. 34. The Argonne Cs137 source was used to do QC on every EBA module.

Because the web was used so extensively for all aspects of production in the US, we provide links which show examples:

[10]QC based on Cs scans: <http://www.hep.anl.gov/ljn/atlasqc.html>

[11]production, qc, and shipping:

<http://www.hep.anl.gov/dgu/ATLAS/optics/production/ANLProduction.html>

[12]links to us production:

http://www.pa.msu.edu/~miller/atlas/optics/us_plant.html

[13]summary plot of us qc: <http://www.pa.msu.edu/~miller/atlas/optics/modules.ps>)



Fig. 33. On the US assembly lines, the glue was injected into the aspirin tubes using a hypodermic needle.

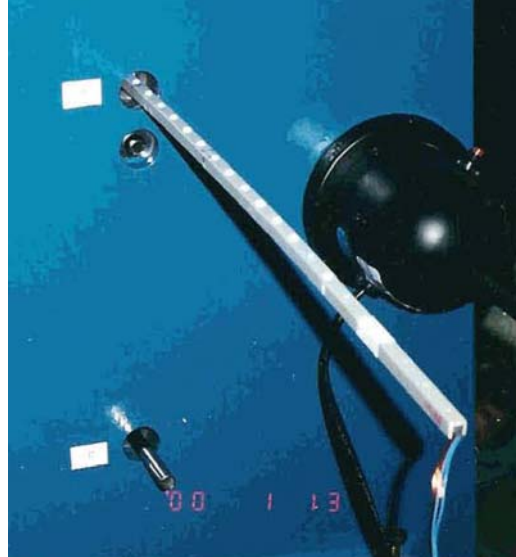


Fig. 34. An LED bar was used to check for mis-routings of fibers. The LED's corresponding to each cell illuminated from each source tube were selected with a microcontroller, and mis-routed fibers were seen visually.

ANL Cs-SOURCE SCAN 521

Run date: 5/21/2002

CELL	LAYER	TILE	%DEV(LJN)	%DEV(BS)	SOLUTION
A12-O	1&3	5	-	-30	Fiber occlusion - REPLACED
A16-E	2	25	-39	-45	Stress-crazed within 1" of sheath (at insertion?) - REPLACED
D5-O	8&10	30	-74/-73	-75	Stress-crazed @ sheath exit (at routing?; near split) - REPLACED
D6-O	8&10	46	-64/-57	-75	No external sign; A/T shows cladding damage signature - REPLACED

Fig. 35. This figure shows a typical list of problems which were found after the first Cs137 scan of a module. This is for module EBA-52. Note that two different, independent analyses of the data were done for each scan. Another scan was done after the repairs listed here were implemented. In this case, no significant problems were found in the second scan.

Overall quality checks on modules at CERN.

For all modules either for the barrel for the Extended Barrels a final check, leading to certification, was taken. For Barrel modules this coincided with the final scan, after all repairs. The instrumented EB modules coming from Spain and the USA were first equipped with Cs source calibration tubes, and then tested with the ^{137}Cs γ -source, repaired if needed and finally subjected to the final certification scan.

The overall quality of the response of all 192 modules is summarized by the estimator of cell uniformity given in Fig. 36. The response of each readout channel (two per cell) of each module is first obtained; it is defined to be the mean of the response of each tile in the cell. Then for each module the RMS deviation from the mean of the cell responses is plotted (one per module) in the figure.

On the basis of simulations of hadron showers in TileCal and of the effect of cell-to-cell response non-uniformities (described in chapter 7 of the TDR [2]) the required cell uniformity was taken to be 10%. It is seen that the uniformity for all the Barrel modules lies in the range of 5-8%. EB modules are less uniform but well below 10% specification.

The observed differences between LB and EB modules, as well as systematic trends in the uniformity of modules within each barrel, which are visible in Fig. 13, are mostly due to the optical quality of the tiles used for the instrumentation. As described in section 2.2, from tile production batch 2 onwards the 50% of the tiles characterized by the highest values of the optical quality estimator were used to instrument LB modules, the remainder were used for the EBs.

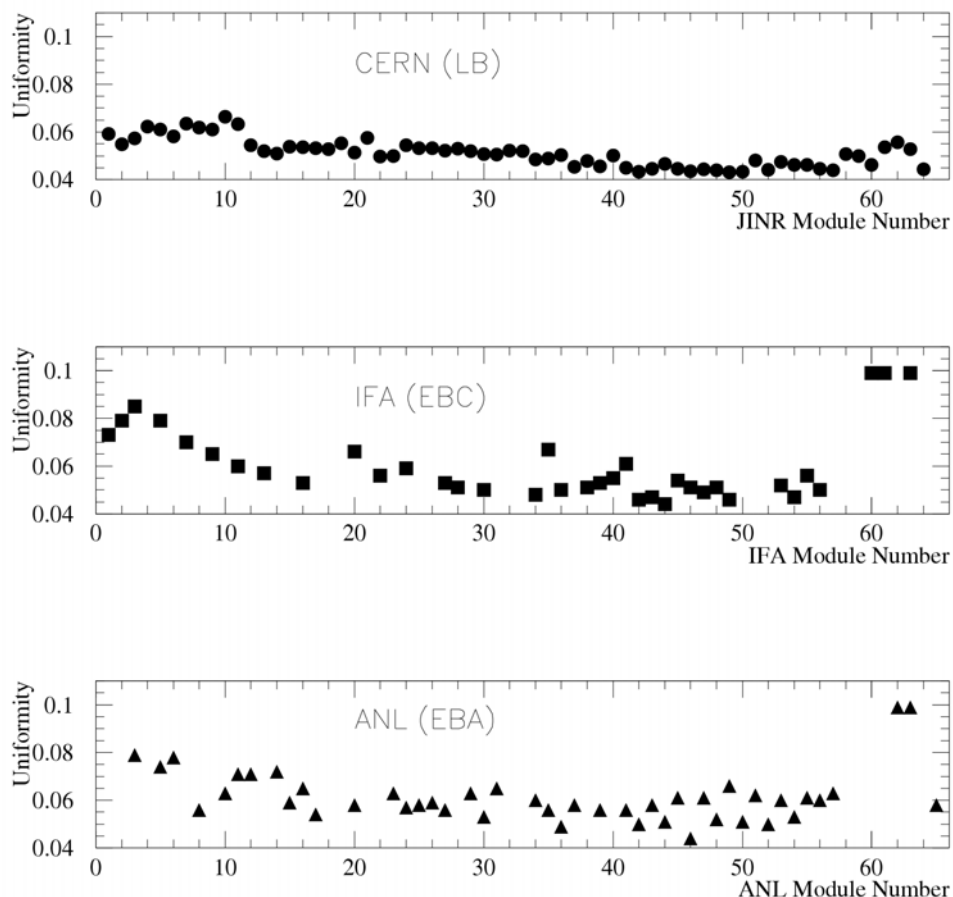


Fig. 36. Cell uniformity as defined in the text for all LB and EB modules.

On top of these differences due to tile optical quality, in Fig. 13 one can appreciate larger differences in the uniformity of EB modules 60 to 64. In these modules, the steel structure and the tiles of several cells of type A were cut to provide space for the supports of the Liquid Argon calorimeter barrels. Consequently the response to the ^{137}Cs source and to particles of these cells is different, and increases the RMS deviations within the affected modules.

It is noted in passing that the certification of barrel modules was done with one of the first super drawers. During the three years of barrel instrumentation (Aug 99 – Sep 02) some components of the super drawer were replaced (PMTs, 3-in-1 cards) and some parameters such as HV settings changed. This did not affect the certification results but led to some irregularities on tile response shown in the Appendix.

6. Acknowledgments

Instrumenting the three barrels of the Tile Calorimeter could never have been done successfully and according to schedule without the highly competent and often original contributions of the technical staff of many Institutes. The quality of their work is attested to by the excellent uniformity of response documented in this Note and is gratefully acknowledged.

References

- [1] ATLAS collaboration, ATLAS Tile Calorimeter Technical Design Report, CERN/LHCC/96-42 (1996).
- [2] Author list, “*Design, Construction and Installation of the ATLAS Hadronic Barrel Scintillator Tile Calorimeter*”, ATL-TILECAL-2007-019.
- [3] A. Gomes *et al.*, “*Cell geometry and fiber lengths of Barrel and Extended Barrel modules*”, ATL-TILECAL-2002-011.
- [4] Author list .., “*The production and qualification of scintillator tiles for the ATLAS hadronic calorimeter TileCal*”, ATL-COM-TILECAL-2007-17.
- [5] M.David *et al.*, “*15 years of experience with quality control of WLS fibres for the ATLAS Tile Calorimeter*”, ATL-COM-TILECAL-2007-022.
- [6] A. Cardeira *et al.*, “*Insertion of 600k WLS optical fibres into 150k plastic channels for the construction of the ATLAS Tile Calorimeter*”, ATL-COM-TILECAL-2007-020.
- [7] J. G. Saraiva *et al.*, “*The aluminization of 600 k WLS fibers for the TileCal/ATLAS/LHC*”, Trans. Nucl. Sci. **51**:1235-1241, 2004.
- [8] E.Starchenko *et al.*, Nucl. Instr. and Meth. A **494** (2002) 381-384, “*Cesium Monitoring System for Atlas Tile Hadron Calorimeter*”. Also ATL- TILECAL-2002-003 .
- [9] A.Karyukhin *et al.*, Nucl. Instr. and Meth. A **508** (2003) 276-286, “*Radioactive source control and electronics for the Atlas tile calorimeter cesium calibration system*”. See also N. Shalanda *et al.*, ATL-TILECAL-98-134.
- [10]QC based on Cs scans: <http://www.hep.anl.gov/ljn/atlasqc.html>
- [11]production, qc, and shipping:
<http://www.hep.anl.gov/dgu/ATLAS/optics/production/ANLProduction.html>
- [12]links to us production:
http://www.pa.msu.edu/~miller/atlas/optics/us_plant.html
- [13]summary plot of us qc:
<http://www.pa.msu.edu/~miller/atlas/optics/modules.ps>)

APPENDICES

A.1 Sorting and masking of tiles for Barrel modules

The tiles used to instrument LB modules at CERN were sorted according to the light yield estimator in two families (normal and extra light yield) to reduce the signal spread within the cells. The extra light yield tiles come from the high light yield tail of the distribution in the given batch; therefore they represent only a small part of the tiles used at CERN.

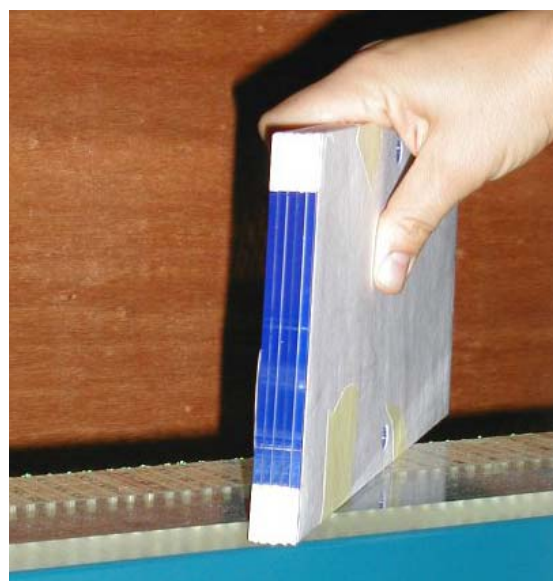
Furthermore, a “masking” procedure was developed in order to reduce the light yield of tiles from Batch 4, which was produced from BASF polystyrene, as described in Section 2.2.

This was necessary where both PSM and BASF tiles had to be used for tile rows belonging to the same readout cell. This turned out to be the case for a number of BC cells, because most of the tiles of size 4, 5 and 6 were made of PSM polystyrene, whereas most of tiles 7, 8 and 9 were made of BASF material.

The tile masking procedure was developed at CERN and consisted of spray-coating part of the readout edges of the high light yield tiles with white diffusive Bicon paint, as shown in Fig. A-1.

The needed length of the painted strips was estimated from the difference in the light yield estimator of the two types of tiles and tested in few cells. For the BC cells, tests of light output reduction were made by coating tiles on both readout sides and at both the inner and the outer radial ends over lengths of 20 mm and 25 mm. This led to choosing to coat the tiles with two symmetric diffusive strips of 22 mm each for the cells containing both PSM and BASF tiles.

Fig. A-1. Masking of tiles by coating part of the edges facing the WLS fibers, at both the inner and outer radial ends. The same strips were painted on the other readout edges of the tiles.



The same procedure was applied for part of the A cells of modules 64 and 65, where PSM and BASF had to be combined. The masking strips were 2 mm x 6 mm and 2 mm x 5 mm respectively.

The overall uniformity plots presented in Section 5 don't show any deterioration of the uniformity for the modules where this masking procedure was systematically applied (barrel modules 15, 16, 18 to 30, 32). This proves the success of the masking procedure.

Further details about the tiles used in the instrumentation process and the sorting and masking procedures are given next.

A cells.

The A cells, the closest to the interaction point in ATLAS, consist of tile rows 1, 2 and 3. The scintillating tiles used to instrument this part of barrel modules come mainly from first two batches and only 2% from the 4th batch. All of them except those from the 4th batch were made of PSM115 polystyrene.

The extra quality tiles were inserted in a few cells of module 32 (A-10, A-9 and A-8) and in all A-cells of modules 45 and 59 (tile rows 2 and 3). In module 45 the increase of the light yield amounts to 5% with respect to the average taken over the cells made of normal quality tiles.

The BASF tiles, which exhibit a 15% higher light yield, were inserted in all cells of module 60 and in some cells of module 61.

Modules 62 and 63 were equipped with PSM tiles left over from EBC instrumentation, corresponding to the lower (about 10%) light yield part of that set.

In some cells of Module 64 and 65, as already remarked, a combination of PSM and masked BASF tiles was used.

BC cells.

The cells consist of tile rows 4-9. Since the tiles were made both of PSM (the whole batch 1 and tile sizes 4-6 of batch 3) and BASF (tile sizes 7-9 of batch 3 and the entire batch 4), one can subdivide the modules into several families according to the light yield of BC cells:

- Modules 1-14, 17 were fully equipped with PSM scintillators.
- Modules 15, 16, 18-30, 32, and part of module 31 (cells BC-7, BC-8, BC-9): PSM scintillators were used in tile rows 4 to 6, and BASF scintillators in rows 7 to 9. For these modules the BASF scintillators of rows 7 to 9 were coated over 2 x 22 mm strips on each readout side as already described.
- The extra-quality tiles entered all the BC-cells in the module 28. This gave a 1% increase of the Cs response comparing to the average of the other modules equipped with PSM tiles.
- Modules 31, 33-65 were instrumented only with the BASF tiles in the BC sampling. In order to maintain a more complete record of tile responses, the gains of the PMTs of the super-drawer used for quality checks were not changed, therefore the BC cells in these modules exhibit a 20% higher Cs response.

D cells

Tile rows 10 and 11 make up the third radial compartment. It was instrumented with PSM tiles (batches 1 and 3) and with the BASF tiles of batch 4, as follows:

- Modules 1-14 and 17 were fully instrumented with PSM tiles.
- Modules 15, 16, 18-65 were equipped with the BASF polystyrene tiles. On the average, the light yield increase of this group with respect to the first one is $\approx 28\%$.
- Module 28 was instrumented with the extra-quality BASF tiles. The light yield was seen to be greater by 2.6% in comparison to that of the other modules equipped with BASF tiles.

Results and summary.

The above mentioned facts about the instrumentation of LB modules are illustrated in Figure A-2, which gives the average responses of tiles in the three cell types normalized to their average for all modules. The irregularities seen in the first 5 modules for all three types of cells are spurious. They are due to the fact that the final setting of PMT gains had not yet been decided.

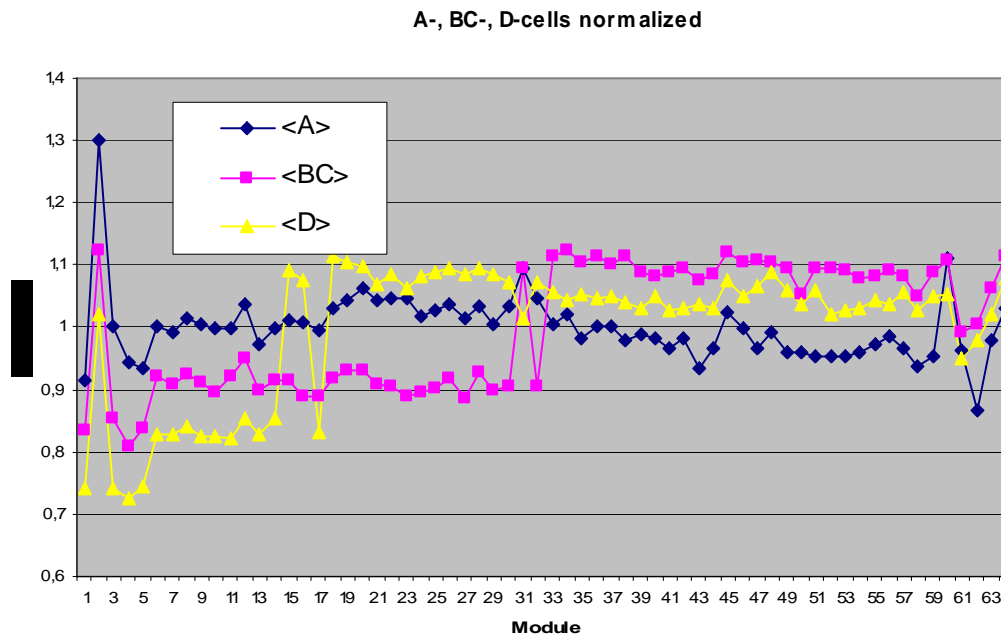


Fig. A-2. Average responses of A; BC and D cells in each LB module, normalized as in text.

In summary, the A-cells except just few modules belong to only one family of responses, the BC-cells belong to two families, as the D-cells. The corresponding modules and the average of Cs response are displayed in table A-1, with the number of cells for each family.

Cell type	Modules	<Cs response>	No. of cells in family 1	No. of cells in family 2
A	1-65	1159	1300	-
BC	1-30,32	1139	558 *	-
	31,33-65	1380	-	612
D	1-14,17	1306	105	-
	15,16,18-65	1669	-	350
Total			1963	962

Table A-1, Illustrating families of Cs responses. Three cells of module 31 are masked (see above). Nevertheless, for simplicity, the BC cells of this module are counted in family 2.

One may also conclude that the light increase due to the extra quality tiles of each batch is very small, whereas the difference between PSM and BASF scintillators is substantial.

A.2 Sorting and masking of tiles for EBC modules

The composition of the EBC modules in terms of PSM vs. BASF tiles is graphically shown in Fig. A-3, which represents what had been done as of February 2002, when four modules had not yet been instrumented but all tiles for these modules were in hand.

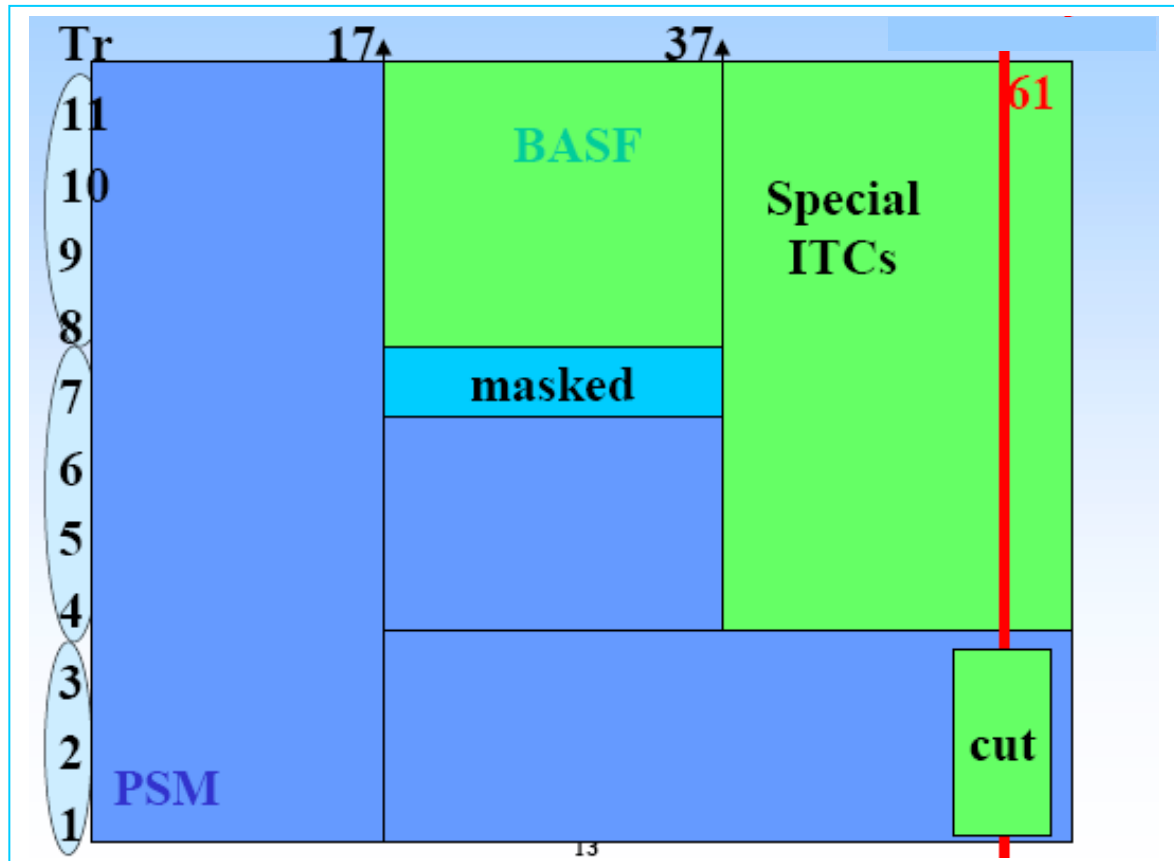


Fig. A-3. Tile materials in the instrumentation of the EBC modules.

PSM tiles were used to instrument all cells of the first 17 modules and for the A-cells of all 64 EBC modules, with the exception of the “cut” A-cells shown in the figure, which as mentioned in Section 5 were cut in order to accommodate the LAr calorimeter supports. The peculiar response of these cells was mentioned in Section 5.

PSM tiles were also used to equip tile rows 4,5 and 6 in modules 18-37. In the EB modules the BC-cells comprise tile rows 4,5,6 and 7, but tiles made of PSM material to equip row 7 of modules beyond 17 was not available. Hence BASF tiles had to be used for tile row 7 of these 20 modules. These tiles were masked by painting two strips of 22.5mm each on the two readout edges of tile7, with the procedure developed at CERN. The loss in the collected light due to the masking was found to be 20% using the ^{137}Cs system at the CERN certification site, 21% using the LED source at the IFAE instrumentation site. At a later time the loss was also measured using 90° test beam muons incident on the geometrical center of masked tiles and was found to be a few percent larger.

The 21% drop in the LED light detected in the IFAE quality control system caused no increase in the RMS spread of signals from the B cell with respect to modules previously instrumented.

All the remaining cells and modules (cells 8 to 11 of modules 18-37; cells 4 to 11 of modules 38-64) were equipped with BASF tiles.

As shown in section 5, the uniformity of cells of EBC modules from 11 onwards is distinctly better than for the earlier ones. This is because until module 10 tiles were inserted into modules without any sorting, whereas later the following improvements were introduced:

- from module 11 onwards, for every tile size the available at IFAE packs of 20 tiles were ordered by the value of the $(I_0 \cdot I_1)^{1/2}$ optical quality estimator, measured for one of the tiles in each pack. Tile packs were then inserted following this order, beginning with the highest value of the tile sample available at the time of instrumenting each module.
- as described in section 2.2, beginning from batch 2 sets of tiles differing in optical quality were destined to each of the three barrels. The EBC instrumentation site received tiles corresponding in optical quality to the third quarter of the $(I_0 \cdot I_1)^{1/2}$ distribution. Tiles were inserted in each row in the order given by this estimator, as was already being done from module 11 on. However the larger samples available at that time produced significantly smaller optical response spreads within each module.

A.3 Sorting and masking of tiles for EBA modules

The tiles used in instrumenting the EBA modules were received in a few batches over the years. As noted, some of these were from a different manufacturer, and had a different intrinsic brightness. The parameters I0 and I1 corresponding to brightness and attenuation had been measured during tile production. These numbers were entered into an Excel spread sheet for sorting in order to match tiles in each cell, and where possible in each row of each module.

A log was then made, to indicate to the instrumentation crews which package of tiles was to go into which slots in a particular module. An example showing a few lines of the sheet are shown below in Fig. A-3. In this instance, tiles from 95 different packages were sorted in order to fill 1451 slots in a module.

Because the BASF tiles were brighter, a masking procedure much like that used on the central barrel was developed for these.

The QC logbooks which record which tile packets went into which module are still preserved at ANL.

MODULE ANL-13

QC-1, 2.2

TILE INSERTION LOG

SIZE	BOX	PACK	IO	START	STOP	SIGNATURE DATE
11						Sally A. 08/03/00
11	14	10	98.6	1	1	
11	50	210	99.5	2	4	
11	11	48	100.1	5	23	
11	61	283	100.9	24	43	

Fig. A-3. A fragment of a Tile insertion log for the EBA modules.